Investigational New Drugs (2019) 37:431–440
https://doi.org/10.1007/s10637-018-0643-4

PRECLINICAL STUDIES

Induction of endoplasmic reticulum stress by aminosteroid derivative RM-581 leads to tumor regression in PANC-1 xenograft model

Martin Perreault[1] · René Maltais[1] · Jenny Roy[1] · Sylvain Picard[2] · Ion Popa[2] · Nicolas Bertrand[3,4] · Donald Poirier[1,5]

Received: 20 April 2018 / Accepted: 13 July 2018 / Published online: 30 July 2018

Summary

The high fatality and morbidity of pancreatic cancer have remained almost unchanged over the last decades and new clinical therapeutic tools are urgently needed. We determined the cytotoxic activity of aminosteroid derivatives RM-133 (androstane) and RM-581 (estrane) in three human pancreatic cancer cell lines (BxPC3, Hs766T and PANC-1). In PANC-1, a similar level of antiproliferative activity was observed for RM-581 and RM-133 (IC_{50} = 3.9 and 4.3 μM, respectively), but RM-581 provided a higher selectivity index (SI = 12.8) for cancer cells over normal pancreatic cells than RM-133 (SI = 2.8). We also confirmed that RM-581 induces the same ER stress-apoptosis markers (*BIP, CHOP* and *HERP*) than RM-133 in PANC-1 cells, pointing out to a similar mechanism of action. Finally, these relevant in vitro results have been successfully translated in vivo by testing RM-581 using different doses (10–60 mg/kg/day) and modes of administration in PANC-1 xenograft models, which have led to tumor regression without any sign of toxicity in mice (animal weight, behavior and histology). Interestingly, RM-581 fully reduced the pancreatic tumor growth when administered orally in mice.

Keywords Aminosteroid · Pancreatic cancer · Endoplasmic reticulum stress aggravator · PANC-1 cells · Mouse xenograft

Abbreviations

AM	Aminosteroid derivative
AUC	Area under the curve
CCAC	Canadian Council on Animal Care
CI	Combination index
C_{max}	Maximal concentration
DMSO	Dimethyl sulfoxide
EDTA	Ethylenediamine tetraacetic acid
ER	Endoplasmic reticulum
HE	Hematoxylin and eosin
IC_{50}	Concentration inhibiting 50% of cell growth
ip	Intraperitoneally
LC/MS/MS	Liquid chromatography/ mass spectrometry/mass spectrometry
MT	Masson's trichrome
MTS	3-(4,5-dimethylthiazol-2-yl)-5-(3-carboxymethoxy-phenyl)-2-(4-sulfophen-yl)-2H-tetrazolium
PAS	Periodic acid Schiff
PAS-D	Periodic acid Schiff with diastase
PBS	Phosphate buffer solution
PG	Propylene glycol
PK	Pharmacokinetic
po	Orally
sc	Subcutaneously
SI	Selectivity index

Martin Perreault and Jenny Roy contributed equally to this work.

Electronic supplementary material The online version of this article (https://doi.org/10.1007/s10637-018-0643-4) contains supplementary material, which is available to authorized users.

✉ Donald Poirier
donald.poirier@crchul.ulaval.ca

[1] Laboratory of Medicinal Chemistry, Endocrinology and Nephrology Unit, CHU de Québec - Research Center (CHUL, T4-42), 2705 Laurier Boulevard, Québec, QC GIV 4G2, Canada

[2] Department of Anatomo-Pathology, CHU de Québec - Université Laval, Québec, QC GIV 4G2, Canada

[3] Faculty of Pharmacy, Université Laval, Québec, QC GIV OA6, Canada

[4] Endocrinology and Nephrology Unit, CHU de Québec-Research Center (CHUL, T4-13), Québec, QC GIV 4G2, Canada

[5] Department of Molecular Medicine, Faculty of Medicine, Université Laval, Québec, QC GIV OA6, Canada

Introduction

In 2017, 53,670 new cases of pancreatic cancer and 43,090 deaths caused by this disease have been predicted for the US population [1]. With a five-year relative survival rate of 8% [1], pancreatic cancer is classified as a high-mortality cancer [2]. Most cancer type survival rates have improved over the last five decades, but pancreatic cancer morbidity has been stable, which illustrates the clinical need for new therapeutic tools to cope with this fatal disease [1].

As a therapeutic approach, endoplasmic reticulum (ER) stress inducers may hold promise to treat pancreatic ductal adenoma carcinoma (PDAC) [3]. Indeed, ER is a predominant organelle in pancreatic cancer cells exposed to a high level of stress from a hostile tumor microenvironment, which is characterized by the presence of reactive oxygen species and low levels of oxygen, nutrients, glucose, and lipids. Thus, the addition of an exogenous stress could be fatal for these cancer cells [4]. In fact, ER stress induces cellular dysfunction that can lead to apoptosis if the level or duration of this stress overpasses the capacity of the unfolding protein response (UPR) to restore cellular homeostasis [5, 6]. Successful examples of molecules targeting ER stress by various ways have been described [7–16] although the use of ER stress-mediated apoptosis for pancreatic cancer treatment is still in infancy. The selectivity of action over normal cells, including pancreatic ones, is another potential advantage of this family of anticancer agents [17].

From structure-activity relationship studies on the anticancer activity of a new family of aminosteroid derivatives (AM) built around an androstane backbone, RM-133 (Fig. 1a) has demonstrated strong in vitro cytotoxic properties on several cancer cell lines, including human PANC-1 pancreatic cancer cells [18–21].

These promising in vitro results were then successfully translated in mice using a PANC-1 cell-derived xenograft model following the subcutaneous (*sc*) administration of RM-133 [22]. However, despite a positive proof-of-concept in a pancreatic cancer model, the metabolic stability of RM-133 was not optimal toward its translation to a clinical setting [23]. Therefore, we hypothesized that the pharmacological properties of RM-133 could be improved by replacing its androstane (C19 steroid) backbone by an estrane one (C18 steroid) like the mestranol core. This modification exemplified by RM-581 (Fig. 1b) advantageously raised the metabolic stability two-fold as well as selectivity for cancerous over normal cells, without losing the anticancer activity [24, 25].

Having improved the metabolic stability of RM-133 by developing the estrane analog RM-581, we are now interested in 1) testing its antiproliferative activity in different pancreatic cancer cell lines; 2) confirming its action as an ER stress aggravator, 3) measuring its plasmatic concentration following an intraperitoneal (*ip*), subcutaneous (*sc*) and oral (*po*) administration, and 4) determining its anticancer efficiency in PANC-1 xenograft mouse models, according to the mode of administration.

Materials and methods

Cell lines

BxPC3, Hs766T and PANC-1 human cancer cell lines were obtained from the American Type Culture Collection (ATCC, Rockville, MD, USA) and routinely grown in RPMI-1640, DMEM and DMEM-F12, respectively, at 37 °C and under 5% CO_2 humidified atmosphere. All medium were obtained from Gibco (Gaithersburg, MD, USA) and were supplemented with L-glutamine (2 mM), antibiotics (100 IU penicillin/ml, 100 μg streptomycin/ml) and 10% (*v*/v) foetal bovine serum. Primary pancreas cells were obtained from CellBiologics (Chicago, IL, USA) and were cultured as per manufacturer recommendation.

Cell proliferation assays, selectivity index (SI) and combination index (CI)

The cell proliferation viability assays were performed using 3-(4,5-dimethylthiazol-2-yl)-5-(3-carboxymethoxyphenyl)-2-(4-sulfophenyl)-2H-tetrazolium (MTS) (Cell Titer 96 Aqueous, Promega, Nepean, ON, Canada) as previously described [18–20]. Cells were plated and allowed to adhere overnight in 96-well plates (10^4 cells/well, in triplicate). RM-581 [9], RM-133 [3] and antineoplastic drugs (provided by the NIH, USA) were dissolved in dimethyl sulfoxide (DMSO), added to cell culture medium, and the cells incubated for 72 h.

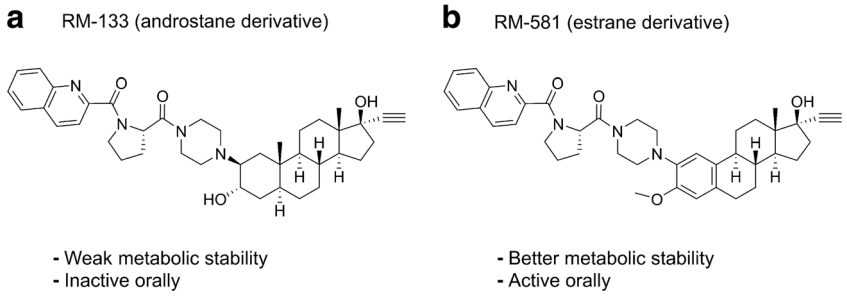

Fig. 1 Chemical structures of aminosteroid derivatives (AM) RM-133 and RM-581

After adding 10 μl of MTS, the cells were incubated for 4 h and the plates were analyzed at 490 nm, using a Tecan M-200 microplate reader (Männedorf, Switzerland). The IC_{50} values (50% of cell growth inhibition) were calculated using GraphPad Prism 6 software. The selectivity index (SI) was calculated by dividing the IC_{50} value obtained for specific primary (normal) cells by the IC_{50} value for the related cancer cell line [26]. The combination index (CI) was calculated using the Chou-Talalay method [27] according to the following formula:

$$CI = \frac{(D)_1}{(D_X)_1} + \frac{(D)_2}{(D_X)_2}$$

Where denominators $(D_x)_l$ and $(D_x)_2$ are the doses of individual drug required to achieve a given effect level and numerators $(D)_1$ and $(D)_2$ are the concentration of each drug present in combination to trigger the same effect level. When the drugs interact additively, CI = 1. CI < 1 indicates a synergistic interaction and CI > 1 indicates an antagonistic effect.

Real time PCR analysis

PANC-1 cells (2.5×10^5) were plated in 6-well plates and treated with 4 μM of RM-581 in a time-course manner. Cells were homogenized in Qiazol buffer (Qiagen, Germantown, MD, USA) and total RNA was extracted according to manufacturer's instructions. RNA concentration was measured using a NanoDrop ND-1000 Spectrophotometer (NanoDrop Technologies, Wilmington, DE, USA). The reverse transcription reaction was performed using 5X All-In-One RT Mastermix (AbmGood, Richmond, BC, Canada) with 1 μg of total RNA at 42 °C for 50 min. cDNA (20 ng) was assessed by fluorescent-based Real time PCR quantification (qPCR), using the CFX384 Touch and SsoAdvanced Universal SYBR Green Supermix (Biorad, Mississauga, ON, Canada). A melting curve was performed to assess non-specific signals. Relative gene expressions were calculated by applying the delta Ct method, using GAPDH as a normalizing gene [28]. Primer sequences are reported in the Supplementary material (Table 1).

Plasma concentration of RM-581 and pharmacokinetic analysis

Six to seven week-old female Balb/c mice were obtained from Charles River Laboratories (Saint-Constant, QC, Canada). Plasmatic concentration of RM-581 was measured at different times, following three different administration modes: *ip* (20 mg/kg), *sc* (60 mg/kg) and *po* (60 mg/kg). RM-581 was synthesized as previously reported [24], dissolved in DMSO, and then added in propylene glycol (PG) to obtain a 8:92 solution. This solution (0.1 ml) was given one time to each mouse (3 mice per group). Blood samples were collected by cardiac puncture at target intervals. They were collected into *Microvette* potassium-EDTA (ethylenediamine tetraacetic acid)-coated tubes (Sarstedt, AG & Co., Numbrecht, Germany) and centrifuged at 3200 rpm for 10 min at 4 °C to obtain the plasma. The concentration of RM-581 was determined by liquid chromatography-mass spectrometry/mass spectrometry (LC-MS/MS) analysis using a procedure developed at the CHU de Québec - Research Center (BioAnalytical Service, CHUL) and described in the Supplementary Data. From these data, the maximum concentration (C_{max}) was obtained while the area under the plasma concentration vs time curve ($AUC_{0\text{-}24h}$) was calculated by the trapezoidal method.

PANC-1 xenograft

Six- to seven-week-old homozygous female *nu/nu* Br athymic mice weighing approximatively 24.7 g were obtained from Charles River Laboratories (Saint-Constant, QC, Canada). PANC-1 cells (5×10^6) were then inoculated *sc* in 0.1 ml of DMEM-F12 medium +30% Matrigel in both flanks of each mouse. After 19 days, the mice were randomly assigned to 7 groups: 1) *ip* control group (3 mice, 6 tumors), 2) *sc* control group (3 mice, 6 tumors), 3) *po* control group (3 mice, 6 tumors), 4) *ip* RM-581 (0.247 mg, 10 mg/kg) (8 mice, 14 tumors), 5) *sc* RM-581 (1.482 mg, 60 mg/kg) (7 mice, 11 tumors), 6) *po* RM-581 (1.482 mg, 60 mg/kg) (7 mice, 11 tumors) and 7) *ip* docetaxel (0.099 mg, 4 mg/kg) (8 mice, 12 tumors). Mice from control groups received the vehicle alone (0.1 ml). RM-581 [24] was dissolved in DMSO (8%) and added in PG (92%), and this solution (0.1 ml) was given 6 days per week. For *sc* administration, RM-581 was injected in the neck, so about 2.5 cm from the tumor site in the flank. Docetaxel (Sigma-Aldrich, Oakville, ON, Canada) was dissolved in DMSO (8%), added to PG (92%), and this solution (0.1 ml) was given 2 times per week. During the treatment (27 days), the tumors were measured twice a week. Two perpendicular diameters were recorded, and tumor area was calculated using the formula L/2 x W/2 x π. The area measured on the first day of treatment was taken as 100%. For more details, see the Supplementary material.

Histological assessment of liver, kidney and intestine toxicity

Tissue samples were rapidly fixed in neutral buffered 10% formalin and processed for routine paraffin embedding. Tissue sections (3 μm) were stained with Haematoxylin and Eosin (HE) and were histologically observed by an independent pathologist. Samples were also stained with Periodic acid - Schiff (PAS) without or with diastase (PAS-D) to demonstrate glycogens, mucins and basal membrane and Masson's

trichrome (MT) and Laidlaw (LA) staining protocols were performed to demonstrate the architectural organization of collagen and argyrophilic reticulum fiber. Digital images at 200X magnification of each slide were obtained using the slide scanner NanoZoomer 2.0-HT (Hamamatsu, Bridgewater, NJ, USA). Whole-section images were visualized using the software NDP view (Hamamatsu, Bridgewater, NJ, USA).

Statistical analysis

Statistical significance was determined according to the Duncan–Kramer multiple-range test [24]. Other differences were evaluated using T-test. *P* values, which were less than 0.05, were considered as statistically significant.

Results

In vitro cytotoxicity and mechanisms of action

To address RM-581's anticancer activity, we conducted a screen involving RM-581, RM-133 (for purposes of comparison) and known antineoplastic drugs (gemcitabine, cisplatin, fluorouracil, oxaliplatin, irinotecan and paclitaxel) (Fig. 2a and Supplementary material – Table 2). Three pancreatic cancer cell lines: BxPC3 [29], PANC-1 [29] and Hs766T [30] were tested in our screening study. In the three cell lines, RM-581 was found to be more cytotoxic compared to the leading clinical chemotherapeutic drug gemcitabine, as well as other alternative drugs, except paclitaxel. Thus, RM-581, RM-133 and paclitaxel displayed similar anticancer activity in PANC-1 cells, but RM-581 was found to be more cytotoxic than RM-133 in BxPC3 and Hs766T cell lines. These results demonstrate the strong in vitro anti-pancreatic cancer activity of RM-581.

The SI for cancer cells over normal cells has been raised with our new lead aminosteroid of estrane series. For RM-581, we indeed previously reported a five-fold increase of SI in breast cancer (MCF-7) cells compared to RM-133 [24]. Therefore, we were interested in comparing the SI of RM-581 and RM-133 in advanced stage pancreatic cancer PANC-1 cells. As for the screen (Fig. 2a), RM-581 and RM-133 have a comparable cytotoxic activity in PANC-1 cells (IC_{50} = 3.9 ± 0.9 μM and 4.3 ± 2.1 μM, respectively) (Fig. 2b). As previously seen for breast cancer cells, RM-581 showed less toxicity for pancreatic primary (normal) cells compared to RM-133, as RM-581 did not affect primary pancreatic cells up to 25 μM, whereas RM-133 displayed an IC_{50} value of 12.1 ± 2.0 μM (Fig. 2b). Therefore, RM-581 has a SI >12.8 in pancreatic cancer cells, which is more than four-fold higher compared to RM-133 (SI = 2.8).

The molecular mechanism of the anticancer action of RM-133 has been investigated and characterized as an ER stress

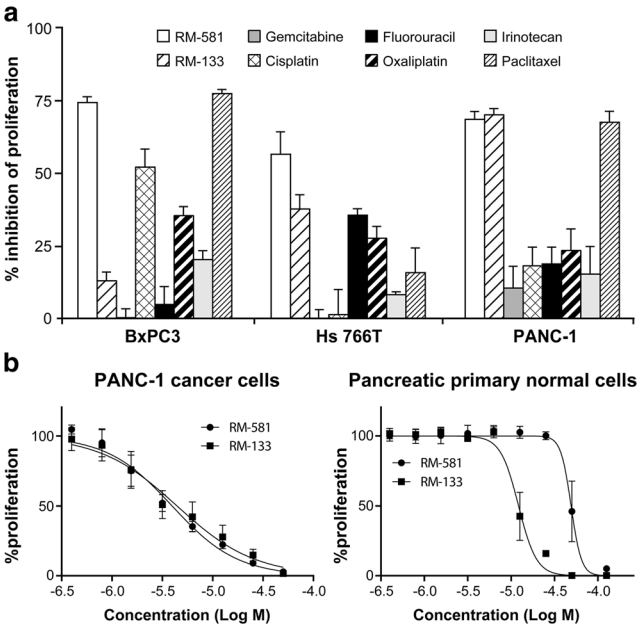

	PANC-1 cells IC_{50} (μM)	Primary pancreatic cells IC_{50} (μM)	Selectivity Index (SI)
RM-581	3.9 ± 0.9	~ 50	~ 12.8
RM-133	4.3 ± 2.1	12.1 ± 2.0	2.8

Fig. 2 RM-581 is toxic for human pancreatic cancer cells and weakly toxic for normal cells. **a** Inhibition of pancreatic cancer cell (BxPC3, Hs766T and PANC-1) proliferation after 72 h of incubation with 5 μM of anticancer drugs. **b** IC_{50} values of RM-581 and RM-133 in pancreatic PANC-1 cancer cells and primary normal cells. Two experiments performed in triplicate ± SD

aggravator causing cancer cell apoptosis [21]. In fact, RM-581 is a mestranol mimic of RM-133 (Fig. 1) with very close structural elements (side chain and steroid core). Thus, considering these similarities, we were interested in confirming the ER stress aggravator action of RM-581. PANC-1 cells were treated in a time-course manner with RM-581 (4 μM) or RM-133 (4 μM) and the transcript level of several markers of intrinsic apoptosis (*BAD*, *BAX*, *BID*, *BCL2* and *CYCS* (cytochrome c)) or ER stress (*BIP*, *CHOP* and *HERP*) were analyzed by qPCR [31, 32]. Treatment of PANC-1 cells with RM-581 did not increase the presence of *BAD*, *BAX*, *BID*, *BCL2* and *CYCS* transcripts (Fig. 3). Therefore, intrinsic apoptosis is clearly not the initial pathway implicated in the mechanism of the anticancer activity of RM-581. In turn, as for RM-133, a treatment of PANC-1 cells with RM-581 considerably raised the presence of *BIP*, *CHOP* and *HERP* transcripts, the classical ER stress-apoptosis markers [21, 33, 34]. From the previous data, RM-581 was confirmed as an ER stress aggravator anticancer drug such as RM-133.

Using the Chou-Talalay method [27], the additive behavior of RM-581 and RM-133 was addressed. This combination experiment in PANC-1 cells demonstrated their additive effect, since the CI values observed equal 1 (Fig. 4a).

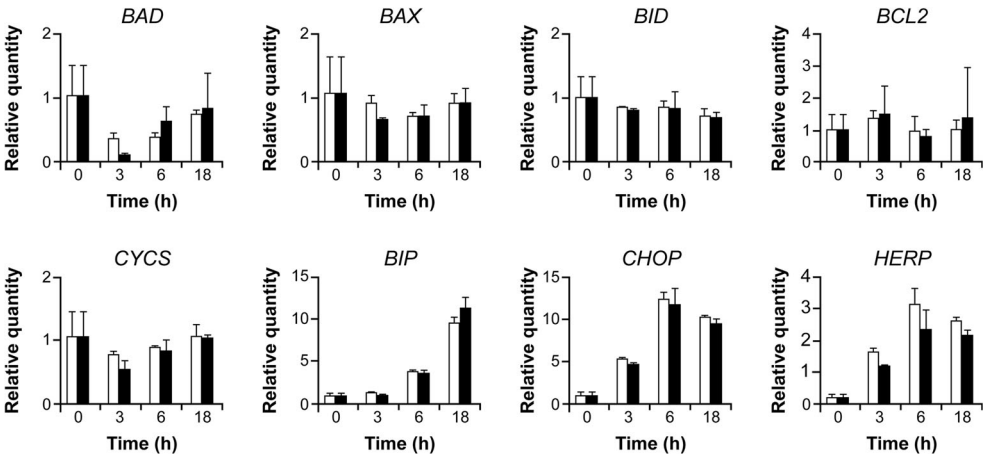

Fig. 3 RM-581 raises the transcription of markers of endoplasmic reticulum stress in PANC-1 cells. qPCR transcript quantification of *BAD*, *BAX*, *BID*, *BCL2*, *CYCS*, *BIP*, *CHOP* and *HERP* in PANC-1 cells treated with 4 μM of RM-581 or RM-133. RM-133: white bars; RM-581: black bars. One experiment performed in triplicate ± SD

Accordingly, a 4 μM combination (50:50) of RM-581 and RM-133 stimulated the presence of *BIP*, *CHOP* and *HERP* transcripts in PANC-1 cells (Fig. 4b). Together, RM-581 and RM-133 are additive in drug combination, which is an additional confirmation pointing out to the same mechanism of action (ER stress aggravator) for these two closely-related AM.

Plasma concentration and pharmacokinetic parameters in mouse

The hepatic microsomal metabolic stability of RM-581 was improved compared to RM-133 [9]. Therefore, the pharmacokinetic (PK) of RM-581 after *ip*, *sc* and *po* administration modes were investigated in the mouse, before the anticancer proof-of-concept. *Ip* administration of 20 mg/kg of RM-581 resulted in a C_{max} of 10,003 ± 855 ng/ml, measured after 15 min. Elimination via this route was quick, with undetectable blood levels of drug after 7 h. The 24-h blood exposure ($AUC_{0\text{-}24h}$) by the *ip* route was around 11,450 ng-h/ml (Fig. 5a).

In comparison, a single *sc* injection of 60 mg/kg of RM-581 resulted in lower blood exposure despite the higher dose ($AUC_{0\text{-}24h}$ = 7758 ng-h/ml), that is approximately 70% of the value obtained with the *ip* injection (Fig. 5b). For comparison, the blood concentration 1 h after the *sc* administration (925 ± 151 ng/ml) were roughly 4-fold below those measured with the *ip* route at the same timepoint. Nevertheless, despite these lower concentrations, the drug remained detectable in the bloodstream up to 24 h after dosing. This suggests a sustained absorption of the *sc* depot, possibly due to the precipitation of the drug upon administration in the confined *sc* compartment. This also suggests that the present experimental design did not allow to fully assess the elimination phase with this injection route.

Interestingly, a 60 mg/kg dose of RM-581 administered *po* resulted in a concentration of 1860 ± 301 ng/ml, 1 h after oral gavage (Fig. 5c). The blood exposure was also considerable ($AUC_{0\text{-}24h}$ = 5545 ng-h/ml), comforting the idea that RM-581 is bioavailable orally. For comparison, the oral gavage of the same dose of RM-133 resulted in much lower blood concentrations (65 ± 21 ng/ml), measured 3 h after dosing. Concentrations of RM-581 at this timepoint were 553 ± 187 ng/ml.

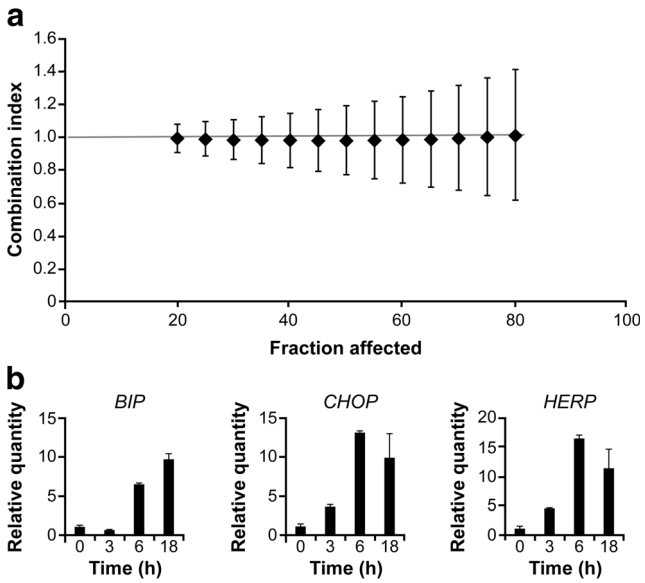

Fig. 4 RM-581 and RM-133 are additive anticancer agents in PANC-1 cells. **a** RM-581 and RM-133 combination index (CI) values were calculated using the Chou-Talalay method. Drug synergy, addition, and antagonism are defined by combination index (CI) values less than 1.0, equal to 1.0, or greater than 1.0, respectively. Two experiments performed in triplicate ± SD. **b** qPCR transcript quantification of *BIP*, *CHOP* and *HERP* in PANC-1 cells treated with 4 μM of a combination (50:50) of RM-581 and RM-133. One experiment performed in triplicate ± SD

PANC-1 xenograft cancer model in mouse

Following the determination of PK parameters, we addressed the ability of RM-581 to block PANC-1 xenograft progression, using three administration modes (*ip*, *sc* and *po*). The C_{max} of RM-581 observed in the *ip* mode (10,003 ng/ml) was about 11-fold higher compared to *sc* mode. Considering that RM-581 has already a 2-fold improved metabolic stability

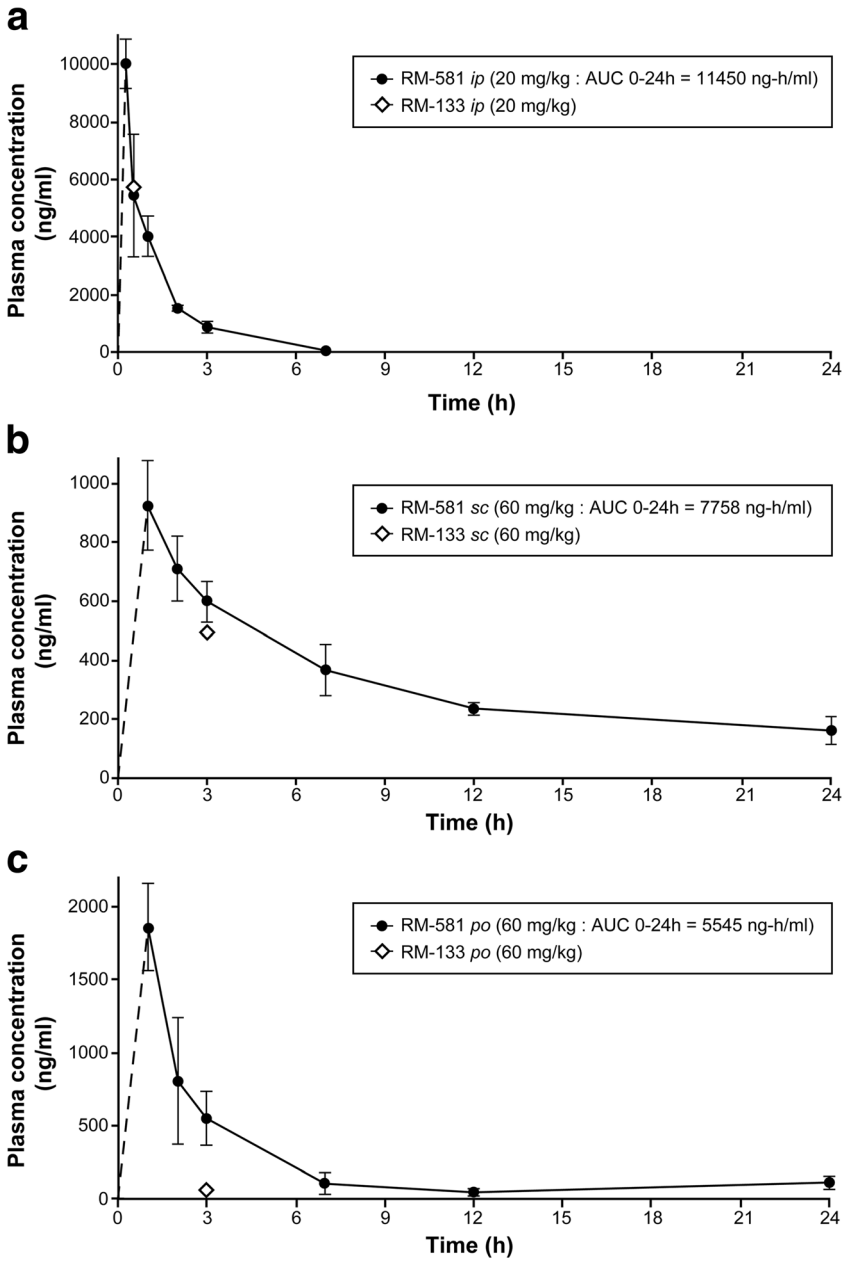

Fig. 5 Pharmacokinetic profiles of a single *ip*, *sc*, and *po* administration of RM-581 in mice. Time course quantification of RM-581 or RM-133 plasma concentrations following a single 20 mg/kg *ip* (**a**), 60 mg/kg *sc* (**b**) or 60 mg/kg *po* (**c**) administration into Balb/c mice. One experiment performed in triplicate ± SEM

over RM-133 [24], we thus decided to use a reduced dose of RM-581 (10 mg/kg) in our *ip* xenograft experiment compared to our previous RM-133 dose (240 mg/kg, *sc*) [22]. Docetaxel (4 mg/kg), administered *ip* twice a week, was used as positive control. RM-581 injected *ip* (6 days a week) produced a significant tumor growth inhibition at day 6 and even a significant regression from initial tumor size at day 20 (Fig. 6a). Interestingly, RM-581 and docetaxel triggered a strong and similar antitumoral effect. Next, we conducted a protocol with *sc* injection in order to compare the efficiency of RM-581 with data previously obtained for RM-133 tested in PANC-1 xenograft [22], which had slow the progression of tumors at 240 mg/kg [22]. Advantageously, compared to RM-133, a *sc* injection of RM-581 (60 mg/kg) provided a significant regression of the tumor size from day 6 and even a significant regression from initial tumor size at day 20 (Fig. 6b). Finally, RM-581 was administered *po* and was found to stop the tumor progression from day 13 and to provoke a significant regression of tumor size from day 23 (Fig. 6c), up to an unmeasurable level due to the small size of the tumors. In summary, RM-581 has been proven to be a more efficient anticancer agent than RM-133 in the PANC-1 xenograft mouse model and, contrary to RM-133, RM-581 inhibits tumor growth when administered orally.

RM-581 demonstrated low toxicity in vitro on normal cells (Fig. 2b) [24]. This safety profile of RM-581 was also confirmed in the present PANC-1 xenograft in vivo mouse experiment, since no body and pancreas weight differences

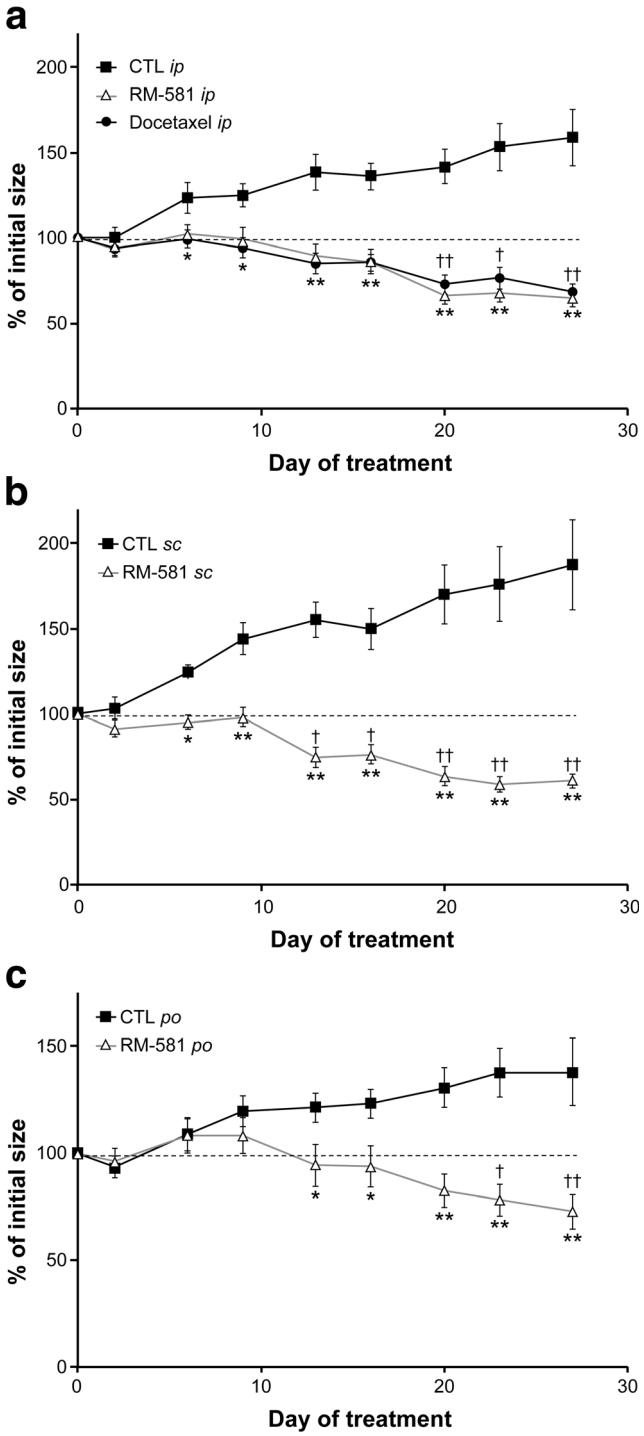

Fig. 6 RM-581 causes tumor regression in PANC-1 mouse xenograft. PANC-1 cells (5×10^6 cells mixed with 30% Matrigel) were inoculated *sc* into both flanks of mice. Tumor-bearing mice were (**a**) injected *ip* with vehicle alone (black square) or RM-581 (10 mg/kg) (green triangle) six day per week or Docetaxel (4 mg/kg) twice a week; (**b**) injected *sc* with vehicle alone (black square) or RM-581 (60 mg/kg) (green triangle) six days per week; (**c**) gavaged *po* with vehicle alone (black square) or RM-581 (60 mg/kg) (green triangle) six days per week. The tumor sizes of mice were recorded twice a week. Data represent the mean ± SEM. RM-581-treated group is significantly different from control group ** ($p < 0.01$), * ($p < 0.05$). Significantly different from day 0 of treatment ++ ($p < 0.01$), + ($p < 0.05$)

were observed between the control group and the groups treated with RM-581 for different administration modes (*ip*, *sc* and *po*) (Supplementary material, Fig. 1. Three tissues of mice treated with RM-581 were also assessed by histology. Thus, hematoxylin and eosin (HE) staining of liver, kidney and small intestine-pancreas tissue samples from mice treated with RM-581 (*ip* and *po*) were analyzed (Fig. 7a, f, j) and their histological examination revealed that liver, kidney and intestine morphology was not affected by the RM-581 treatment. To further validate that RM-581 is non-toxic for the liver, kidneys, intestine and pancreas, we carried out Laidlaw, PAS, PAS-D and Masson's trichrome (MT) staining (Fig. 7b, c, d, e, f, g, h, i). Again, analyses confirmed that RM-581 is non-toxic for major drug-toxicity targeted organs [35–37]. Together, these results confirmed that the observed selectivity of RM-581 for cancer cells over normal cells was translated in vivo.

Discussion

In order to demonstrate the advantageous anti-pancreatic cancer activity of RM-581, a screening assay at two concentrations (1 and 5 μM) was performed including RM-133 and antineoplastic agents used in a clinical setting; namely: gemcitabine [38], cisplatin [39], fluorouracil [40], oxaliplatin [41], irinotecan [41] and paclitaxel. RM-581, RM-133 and antineoplastic drugs were tested in three pancreatic cancer cell lines (BxPC3, Hs766T and PANC-1). Except for paclitaxel, RM-581 was found to be significantly more active compared to the selected chemotherapeutic agents in the three cancer cell lines (Fig. 2a). Importantly, these cell lines are known to be resistant to gemcitabine [42, 43]. As this resistance is linked to high phosphorylated extracellular signal regulated kinase (pERK) expression in BxPC3 and PANC-1 cells [42], our results suggest that this oncogenic event cannot lead to RM-581 resistance to these cancer cells. Together, RM-581 has demonstrated a high anticancer efficiency in vitro in BxPC3, Hs766T and PANC-1 cells, and could represent a valuable therapeutic alternative for these gemcitabine-resistant cell lines.

An extensive study aiming at characterizing the molecular mechanism governing the anticancer activity of RM-133 has classified this aminosteroid as an ER stress aggravator that causes cancer cell apoptosis [21]. The chemical structure of RM-581 and RM-133 are very similar, being distinguishable only by the nature of the A-ring of their steroidal backbone. In fact, RM-581 could be viewed as a mestranol mimic of the androstane RM-133 (Fig. 1), conferring it a potential advantage for metabolic stability [24]. Despite these close structural similitudes, we were however interested in confirming their similar

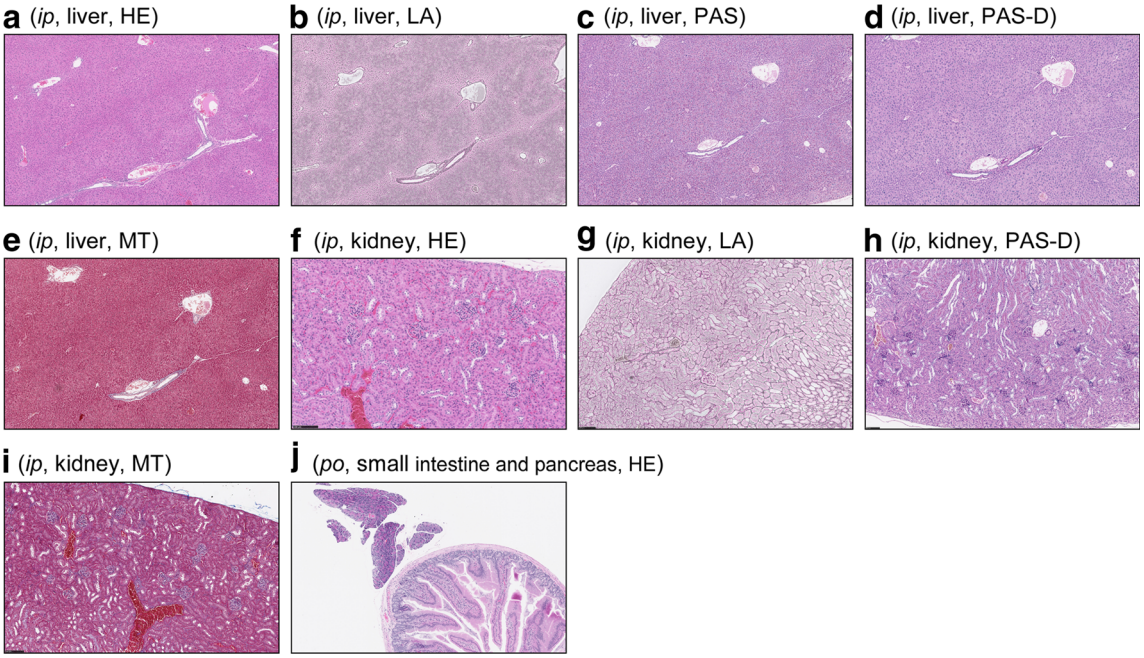

Fig. 7 Liver, kidney and intestine samples of mice treated 27 days with RM-581 are not displaying histological signs of toxicity. **a** Hematoxylin and eosin (HE), **b** Laidlaw (LA), **c** PAS, **d** PAS-D or **e** Masson's trichrome (MT) staining of liver slices of mouse treated with RM-581 (10 mg/kg *ip*) (200X magnification). **f** HE, **g** LA, **h** PAS-D or **i** MT staining of kidney slices of mouse treated with RM-581 (10 mg/kg *ip*) (200X magnification). **j** HE staining of intestines/pancreas slice of mouse treated with RM-581 (60 mg/kg *po*) (200X magnification)

mechanisms of action, and their effects on pancreatic cancer cells, considering that small structural changes could sometimes have dramatic consequences on a given activity. We therefore addressed the classical gene transcripts for the intrinsic apoptosis and the ER stress-apoptosis pathways by qPCR in PANC-1, treated with 4 μM of RM-133 or RM-581 (Fig. 3). As expected, and previously obtained in HL-60 cells, RM-133 did not stimulate the transcription of the intrinsic apoptosis markers *BAD*, *BAX*, *BID*, *BCL2* and *CYCS* [31], but strongly raised the presence of the ER stress-apoptosis markers *BIP*, *CHOP* and *HERP* [21, 24, 32]. Therefore, RM-581 is also classified as an ER stress aggravator anticancer molecule. As a complementary experiment to confirm the similar mechanism of action pattern of these AM, we next demonstrated their additive effect on PANC-1 (Fig. 4a). Accordingly, the combination of the two aminosteroids triggered the same effect on the transcription of intrinsic apoptosis and ER stress-apoptosis markers, which at the molecular level, suggest that RM-133 and RM-581 trigger their anticancer activity in an additive manner, via the same molecular mechanism (Fig. 4b).

We next addressed the pharmacokinetic behavior of RM-581 in mice. In the same *sc* experimental design, RM-133 reached a C_{max} of 390 ng/ml at 3 h [22], but RM-581 reached a C_{max} of 925 ng/ml at 1 h and a plasma concentration of 598 ng/ml at 3 h (Fig. 5b). This raise in plasma concentration for the same mode of administration *sc*, in combination with the better metabolic stability of RM-581 [24], can explain its anticancer efficiency in PANC-1 xenograft models, compared to RM-133, even if both aminosteroid have similar IC_{50} values in PANC-1 cell viability assays. In fact, RM-581 triggered a tumor size regression (Fig. 6), whereas RM-133 only slowed tumor progression in a previous experiment [22]. Thus, *ip* and *sc* treatments with RM-581 reached significant tumor regression before the one observed with *po* treatment (day 6 vs day 13). In fact, at the same dose of 60 mg/kg, the plasma concentration level of the *po* mode decreased more rapidly than in the *sc* mode, with a complete clearance after 12 h, but the $AUC_{0\text{-}24h}$ values were not so different (7758 and 5545 ng-h/ml for *sc* and *po*, respectively) (Fig. 5). This observation could be explained by the lipophilicity of RM-581, which is compatible with a *sc* injection that generate a slow and a more constant release of this aminosteroid daily. Therefore, both *sc* and *po* administration schedule or formulation could be further optimized to reach optimal benefit. However, it is important to mention that contrary to RM-133, RM-581 is fully active when administered orally by gavage (*po*).

As the in vitro primary cell model for predicting drug toxicity is often uncertain [44], we completed our toxicology evaluation of RM-581 adverse effects using tissue slice visualization. Histological examination of mouse liver and kidney, two of the organs most affected by drug toxicity [35, 36] did not have any sign of toxicity after an *ip* treatment of mice with RM-581 for 27 days. Moreover, intestines of mice orally treated with RM-581 *po* were also not affected by the treatment. Together, our in vitro and in vivo toxicological results

demonstrate that RM-581 is a selective anticancer molecule for cancer cells, over normal cells.

Conclusion

The results presented herein demonstrate that the aminosteroid RM-581 is a promising anticancer molecule. Anticancer activity has been observed for RM-581 in different gemcitabine-resistant pancreatic cancer cell lines. RM-581 was then classified as an ER stress aggravator anticancer pro-apoptotic drug, which confers to this steroidal derivative an interesting selective action on cancer pancreatic cells over normal cells. These in vitro results were successfully translated in vivo in a PANC-1 cell-derived xenograft model for three modes of administration (*ip*, *sc* and *po*). Contrary to RM-133, RM-581 has been proven to be an active anticancer molecule that can be administered orally. Altogether, these results qualified RM-581 as a valuable preclinical candidate to be further evaluated in a pancreatic cancer clinical phase 1 trial.

Acknowledgments We thank Sonia Francoeur (animal facilities) and Patrick Caron (LC-MS/MS analyses) for their technical assistance. We would also like to thank Micheline Harvey for careful reading of the manuscript, and The National Institutes of Health (Bethesda, MD, USA) for providing the antineoplastic drugs.

Funding This work was supported by the Canadian Institutes of Health Research (CIHR) from the Targeting High Fatality Cancers – Innovation Grant program and the Proof of Principle-Phase I program.

Compliance with ethical standards

Conflict of interest MP, RM, JR and DP have ownership interests on patent applications and patents related to these families of aminosteroid derivatives. SP, IP and NB declare no conflict of interest.

References

1. Cancer Facts & Figures 2017 - American Cancer Society. (2017)
2. Midha S, Chawla S, Garg PK (2016) Modifiable and non-modifiable risk factors for pancreatic cancer: a review. Cancer Lett 381:269–277. https://doi.org/10.1016/j.canlet.2016.07.022
3. Ergin K, Gökmen E (2015) Endoplasmic reticulum stress and pancreatic cancer. Meandros Med Dent J 16:20–24. https://doi.org/10.5152/adutfd.2015.1871
4. Riha R, Gupta-Saraf P, Bhanja P, Badkul S, Saha S (2017) Stressed out - therapeutic implications of ER stress related cancer research. Oncomedicine 2:156–167. https://doi.org/10.7150/oncm.22477
5. Sano R, Reed JC (2013) ER stress-induced cell death mechanisms. Biochim Biophys Acta 1833:3460–3470. https://doi.org/10.1016/j.bbamcr.2013.06.028
6. Tabas I, Ron D (2011) Integrating the mechanisms of apoptosis induced by endoplasmic reticulum stress. Nat Cell Biol 13:184–190. https://doi.org/10.1038/ncb0311-184
7. Hu Y, Zhao C, Zheng H, Lu K, Shi D, Liu Z, Dai X, Zhang Y, Zhang X, Hu W, Liang G (2017) A novel STAT3 inhibitor HO-3867 induces cell apoptosis by reactive oxygen species-dependent endoplasmic reticulum stress in human pancreatic cancer cells. Anti-Cancer Drugs 28:392–400. https://doi.org/10.1097/cad.0000000000000470
8. Cheng S, Swanson K, Eliaz I, McClintick JN, Sandusky GE, Sliva D (2015) Pachymic acid inhibits growth and induces apoptosis of pancreatic cancer in vitro and in vivo by targeting ER stress. PLoS One 10:e0122270. https://doi.org/10.1371/journal.pone.0122270
9. Nawrocki ST, Carew JS, Pino MS, Highshaw RA, Dunner K Jr, Huang P, Abbruzzese JL, McConkey DJ (2005) Bortezomib sensitizes pancreatic cancer cells to endoplasmic reticulum stress-mediated apoptosis. Cancer Res 65:11658–11666. https://doi.org/10.1158/0008-5472.can-05-2370
10. Ranjan A, German N, Mikelis C, Srivenugopal K, Srivastava SK (2017) Penfluridol induces endoplasmic reticulum stress leading to autophagy in pancreatic cancer. Tumour Biol 39(6). https://doi.org/10.1177/1010428317705517
11. Lin S, Zhang J, Chen H, Chen K, Lai F, Luo J, Wang Z, Bu H, Zhang R, Li H, Tong H (2013) Involvement of endoplasmic reticulum stress in capsaicin-induced apoptosis of human pancreatic cancer cells. Evid Based Complement Alternat Med 2013:629750. https://doi.org/10.1155/2013/629750
12. Mujumdar N, Banerjee S, Chen Z, Sangwan V, Chugh R, Dudeja V, Yamamoto M, Vickers SM, Saluja AK (2014) Triptolide activates unfolded protein response leading to chronic ER stress in pancreatic cancer cells. Am J Physiol Gastrointest Liver Physiol 306:G1011–G1020. https://doi.org/10.1152/ajpgi.00466.2013
13. Carracedo A, Gironella M, Lorente M, Garcia S, Guzman M, Velasco G, Iovanna JL (2006) Cannabinoids induce apoptosis of pancreatic tumor cells via endoplasmic reticulum stress-related genes. Cancer Res 66:6748–6755. https://doi.org/10.1158/0008-5472.can-06-0169
14. Gajate C, Matos-da-Silva M, Dakirel H, Fonteriz RI, Alvarez J, Mollinedo F (2012) Antitumor alkyl-lysophospholipid analog edelfosine induces apoptosis in pancreatic cancer by targeting endoplasmic reticulum. Oncogene 31:2627–2639. https://doi.org/10.1038/onc.2011.446
15. Lei P, Abdelrahim M, Cho SD, Liu X, Safe S (2008) Structure-dependent activation of endoplasmic reticulum stress-mediated apoptosis in pancreatic cancer by 1,1-bis(3′-indoly)-1-(p-substituted phenyl)methanes. Mol Cancer Ther 7:3363–3372. https://doi.org/10.1158/1535-7163.mct-08-0439
16. Abdelrahim M, Newman K, Vanderlaag K, Samudio I, Safe S (2006) 3,3′-diindolylmethane (DIM) and its derivatives induce apoptosis in pancreatic cancer cells through endoplasmic reticulum stress-dependent upregulation of DR5. Carcinogenesis 27:717–728. https://doi.org/10.1093/carcin/bgi270
17. Chien W, Ding LW, Sun QY, Torres-Fernandez LA, Tan SZ, Xiao J, Lim SL, Garg M, Lee KL, Kitajima S, Takao S, Leong WZ, Sun H, Tokatly I, Poellinger L, Gery S, Koeffler PH (2014) Selective inhibition of unfolded protein response induces apoptosis in pancreatic cancer cells. Oncotarget 5:4881–4894. https://doi.org/10.18632/oncotarget.2051
18. Ayan D, Maltais R, Hospital A, Poirier D (2014) Chemical synthesis, cytotoxicity, selectivity and bioavailability of 5alpha-androstane-3alpha,17beta-diol derivatives. Bioorg Med Chem 22:5847–5859. https://doi.org/10.1016/j.bmc.2014.09.026
19. Roy J, Maltais R, Jegham H, Poirier D (2011) Libraries of 2beta-(N-substituted piperazino)-5alpha-androstane-3alpha, 17beta-diols: chemical synthesis and cytotoxic effects on human leukemia HL-60 cells and on normal lymphocytes. Mol Divers 15:317–339. https://doi.org/10.1007/s11030-010-9273-2
20. Jegham H, Roy J, Maltais R, Desnoyers S, Poirier D (2012) A novel aminosteroid of the 5alpha-androstane-3alpha,17beta-diol family induces cell cycle arrest and apoptosis in human promyelocytic

leukemia HL-60 cells. Investig New Drugs 30:176–185. https://doi.org/10.1007/s10637-010-9548-6
21. Perreault M, Maltais R, Kenmogne LC, Létourneau D, Gobeil S, LeHoux JG, Poirier D (2018) Implication of STARD5 and cholesterol homeostasis disturbance in the endoplasmic reticulum stress-related response induced by pro-apoptotic aminosteroid RM-133. Pharmacol Res 128:52–60
22. Kenmogne LC, Ayan D, Roy J, Maltais R, Poirier D (2015) The aminosteroid derivative RM-133 shows in vitro and in vivo antitumor activity in human ovarian and pancreatic cancers. PLoS One 10(12):e0144890. https://doi.org/10.1371/journal.pone.0144890
23. Perreault M, Maltais R, Dutour R, Poirier D (2016) Explorative study on the anticancer activity, selectivity and metabolic stability of related analogs of aminosteroid RM-133. Steroids 115:105–113. https://doi.org/10.1016/j.steroids.2016.08.015
24. Perreault M, Maltais R, Roy J, Dutour R, Poirier D (2017) Design of a mestranol 2-N-piperazino-substituted derivative showing potent and selective in vitro and in vivo activities in MCF-7 breast cancer models. ChemMedChem 12:177–182. https://doi.org/10.1002/cmdc.201600482
25. Dutour R, Maltais R, Perreault M, Roy J, Poirier D (2018) Parallel solid-phase synthesis using a new diethylsilylacetylenic linker and leading to mestranol derivatives with potent antiproliferative activities on multiple cancer cell lines. Anti Cancer Agents Med Chem (in press)
26. Haglund C, Aleskog A, Nygren P, Gullbo J, Hoglund M, Wickstrom M, Larsson R, Lindhagen E (2012) In vitro evaluation of clinical activity and toxicity of anticancer drugs using tumor cells from patients and cells representing normal tissues. Cancer Chemother Pharmacol 69:697–707. https://doi.org/10.1007/s00280-011-1746-1
27. Chou TC (2010) Drug combination studies and their synergy quantification using the Chou-Talalay method. Cancer Res 70:440–446. https://doi.org/10.1158/0008-5472.CAN-09-1947
28. Pfaffl MW (2001) A new mathematical model for relative quantification in real-time RT-PCR. Nucleic Acids Res 29(9):e45
29. Nambiar D, Prajapati V, Agarwal R, Singh RP (2013) In vitro and in vivo anticancer efficacy of silibinin against human pancreatic cancer BxPC-3 and PANC-1 cells. Cancer Lett 334:109–117. https://doi.org/10.1016/j.canlet.2012.09.004
30. Marchesi F, Monti P, Leone BE, Zerbi A, Vecchi A, Piemonti L, Mantovani A, Allavena P (2004) Increased survival, proliferation, and migration in metastatic human pancreatic tumor cells expressing functional CXCR4. Cancer Res 64:8420–8427. https://doi.org/10.1158/0008-5472.can-04-1343
31. Kiraz Y, Adan A, Kartal Yandim M, Baran Y (2016) Major apoptotic mechanisms and genes involved in apoptosis. Tumour Biol 37:8471–8486. https://doi.org/10.1007/s13277-016-5035-9
32. Sopha P, Ren HY, Grove DE, Cyr DM (2017) Endoplasmic reticulum stress-induced degradation of DNAJB12 stimulates BOK accumulation and primes cancer cells for apoptosis. J Biol Chem 292:11792–11803. https://doi.org/10.1074/jbc.M117.785113
33. Nagelkerke A, Bussink J, Sweep FC, Span PN The unfolded protein response as a target for cancer therapy. Biochim Biophys Acta 1846:277–284. https://doi.org/10.1016/j.bbcan.2014.07.006
34. Wang M, Kaufman RJ (2014) The impact of the endoplasmic reticulum protein-folding environment on cancer development. Nat Rev Cancer 14:581–597. https://doi.org/10.1038/nrc3800
35. Luo G, Shen Y, Yang L, Lu A, Xiang Z (2017) A review of drug-induced liver injury databases. Arch Toxicol 91:3039–3049. https://doi.org/10.1007/s00204-017-2024-8
36. Awdishu L, Mehta RL (2017) The 6R's of drug induced nephrotoxicity. BMC Nephrol 18(1):124. https://doi.org/10.1186/s12882-017-0536-3
37. Jain AK, Jain S (2016) Advances in oral delivery of anti-cancer prodrugs. Expert Opin Drug Deliv 13:1759–1775. https://doi.org/10.1080/17425247.2016.1200554
38. Lamb YN, Scott LJ (2017) Liposomal irinotecan: a review in metastatic pancreatic adenocarcinoma. Drugs 77:785–792. https://doi.org/10.1007/s40265-017-0741-1
39. Sahin IH, Lowery MA, Stadler ZK, Salo-Mullen E, Iacobuzio-Donahue CA, Kelsen DP, O'Reilly EM (2016) Genomic instability in pancreatic adenocarcinoma: a new step towards precision medicine and novel therapeutic approaches. Expert Rev Gastroenterol Hepatol 10:893–905. https://doi.org/10.1586/17474124.2016.1153424
40. Vogel A, Ciardiello F, Hubner RA, Blanc JF, Carrato A, Yang Y, Patel DA, Ektare V, de Jong FA, Gill S (2016) Post-gemcitabine therapy for patients with advanced pancreatic cancer - a comparative review of randomized trials evaluating oxaliplatin- and/or irinotecan-containing regimens. Cancer Treat Rev 50:142–147. https://doi.org/10.1016/j.ctrv.2016.09.001
41. Kamisawa T, Wood LD, Itoi T, Takaori K (2016) Pancreatic cancer. Lancet 388:73–85. https://doi.org/10.1016/S0140-6736(16)00141-0
42. Fryer RA, Barlett B, Galustian C, Dalgleish AG (2011) Mechanisms underlying gemcitabine resistance in pancreatic cancer and sensitisation by the iMiD lenalidomide. Anticancer Res 31:3747–3756
43. Wennier ST, Liu J, Li S, Rahman MM, Mona M, McFadden G (2012) Myxoma virus sensitizes cancer cells to gemcitabine and is an effective oncolytic virotherapeutic in models of disseminated pancreatic cancer. Mol Ther 20:759–768. https://doi.org/10.1038/mt.2011.293
44. Zhang C, Ball J, Panzica-Kelly J, Augustine-Rauch K (2016) In vitro developmental toxicology screens: a report on the progress of the methodology and future applications. Chem Res Toxicol 29:534–544. https://doi.org/10.1021/acs.chemrestox.5b00458